Journal of Mechatronics, Electrical Power, and Vehicular Technology 13 (2022) 60-71

Journal of Mechatronics, Electrical Power, and Vehicular Technology

CrossMark

e-ISSN: 2088-6985
p-ISSN: 2087-3379

mev.lipi.go.id

State of charge estimation of ultracapacitor based on equivalent circuit model using adaptive neuro-fuzzy inference system

Rizal Nurdiansyah [a, *], Novie Ayub Windarko [a], Renny Rakhmawati [a], Muhammad Abdul Haq [b]

[a] *Electrical Engineering Department, Politeknik Elektronika Negeri Surabaya Jl. Raya ITS, Surabaya, 60111, Indonesia*

[b] *Department of Electrical Engineering and Computer Science, Tokyo Metropolitan University 1-1 Minami-Osawa, Hachioji-shi, Tokyo, 192-0397, Japan*

Received 31 May 2022; 1st revision 23 June 2022; 2nd revision 28 June 2022; Accepted 29 June 2022; Published online 29 July 2022

Abstract

Ultracapacitors have been attracting interest to apply as energy storage devices with advantages of fast charging capability, high power density, and long lifecycle. As a storage device, accurate monitoring is required to ensure and operate safely during the charge/discharge process. Therefore, high accuracy estimation of the state of charge (SOC) is needed to keep the Ultracapacitor working properly. This paper proposed SOC estimation using the Adaptive Neuro-Fuzzy Inference System (ANFIS). The ANFIS is tested by comparing it to true SOC based on an equivalent circuit model. To find the best method, the ANFIS is modified and tested with various membership functions of triangular, trapezoidal, and gaussian. The results show that triangular membership is the best method due to its high accuracy. An experimental test is also conducted to verify simulation results. As an overall result, the triangular membership shows the best estimation. Simulation results show SOC estimation mean absolute percentage error (MAPE) is 0.70 % for charging and 0.83 % for discharging. Furthermore, experimental results show that MAPE of SOC estimation is 0.76 % for random current. The results of simulations and experimental tests show that ANFIS with a triangular membership function has the most reliable ability with a minimum error value in estimating the state of charge on the Ultracapacitor even under conditions of indeterminate random current.

Keywords: Ultracapacitors; state of charge; adaptive neuro-fuzzy inference system; energy storage devices; equivalent circuit model.

I. Introduction

Ultracapacitors (UCs), also known as Supercapacitors (SCs) or electric double-layer capacitors (EDLC), are now increasingly being used in electrical applications as energy storage devices. An Ultracapacitor is a type of electric double-layer capacitor with a broad operating temperature range, low internal resistance, excellent durability, high power density, and high discharge capability to supply peak power requirements [1][2]. The use of Ultracapacitors as energy storage devices is currently being increasingly used in electrical applications such as hybrid energy storage systems (HESS), electric vehicles (EVs), powertrains, and several other electrical applications [3][4][5]. The limitations of batteries in electric vehicles are their limited life cycle, low discharge rates, and special techniques needed to extend their life [6][7]. The latest solution to overcome this problem is to use an Ultracapacitor as an additional power source for the main propulsion of electric vehicles and as a source of electrical energy in regenerative braking, which requires a short time [8]. Ultracapacitor has fast charging capability with a charging current of up to tens of amperes and high discharge capability with a maximum discharge current of up to hundreds of amperes in one cycle [9]. Fast charging capability is supported by the discovery of new materials with nanostructures, making the Ultracapacitor has a larger capacitance even though its energy density is

* Corresponding Author. Tel: +62 858 5150 3369
E-mail address: nurdiansyahrizal@pe.student.pens.ac.id

doi: https://dx.doi.org/10.14203/j.mev.2022.v13.60-71
2088-6985 / 2087-3379 ©2022 National Research and Innovation Agency

MEV is Scopus indexed Journal and accredited as Sinta 1 Journal (https://sinta.kemdikbud.go.id/journals/detail?id=814)
How to Cite: R. Nurdiansyah *et al.*, "State of charge estimation of ultracapacitor based on equivalent circuit model using adaptive neuro-fuzzy inference system," *Journal of Mechatronics, Electrical Power, and Vehicular Technology*, vol. 13, no. 1, pp. 60-71, July 2022.

not greater than that of a lithium-ion battery [10]. Ultracapacitors can be used in extreme temperatures because they have a wide operating temperature range and are supported by long cycle life, giving them an advantage over other energy storage devices [11]. Technological developments increasingly encourage Ultracapacitor, which has many advantages as an energy storage device to replace batteries [12].

In their implementation, some utilize Ultracapacitor-battery hybrids to get optimal performance from both energy storage devices [13]. It is also possible to use an Ultracapacitor as the primary energy storage device in electric vehicles, for example, electric scooters and buses [14]. Fast charging capabilities make Ultracapacitor a breakthrough in battery replacement technology [15]. The power supply for driving electric vehicles with high traction encourages using Ultracapacitors with the advantages of high-power density and super-fast charging [16]. The high efficiency of the Ultracapacitor is due to the low resistance of the constituent material supported by a high-power density, which makes it capable of high current discharge and low power dissipation [17]. The Ultracapacitor's life cycle is much longer than other energy storage devices. The level of security using Ultracapacitor needs to be considered with SOC monitoring [18].

The conventional method for determining the state of charge is the open-circuit voltage (OCV) method which requires a rest period to determine the original voltage on the Ultracapacitor, so it is not possible to use it in practical applications. The weakness of the OCV method cannot be measured in an operating state because an effective measurement when the condition is the voltage at the terminals does not represent the open-circuit voltage in the energy storage [19]. The use of coulomb counting only uses current operating parameters without regard to the internal conditions of the Ultracapacitor and requires measuring instruments with high accuracy to avoid periodic errors. The Unscented Kalman Filter (UKF) application for SOC estimation still requires OCV-SOC mapping to obtain accurate information about SOC, and complex modeling makes parameter identification more difficult [20]. The difference between Ultracapacitors and other energy storage devices is the ability to have a deeper discharge depth to be used optimally [21].

Accurate state of charge (SOC) monitoring is one of the factors in maintaining the safety of Ultracapacitor performance to avoid overcharge or over-discharge conditions that cause dangerous conditions when used. Ultracapacitor modeling is needed to determine its characteristics and electrical behavior so that it has high accuracy in determining the state of charge. The Kalman Filter method uses a more complex equation to get the state of charge value. Based on experiments, estimates with the Kalman Filter have an error reading of about 5 % [22]. Several models analyze the original characteristics of Ultracapacitors, including classical equivalent circuit models, dynamic models, and transmission models [23][24]. The modeling that represents the characteristics of the Ultracapacitor is a combination of series resistors and capacitors with the addition of parallel resistors as self-discharge modeling [25][26]. This paper proposes modeling with a combination of resistor and capacitor components as the relevant model and is referred to as the equivalent circuit model (ECM). The proper modeling will get the process of monitoring the state of charge (SOC) on the Ultracapacitor. By modeling the equivalent circuit models, which are simple and relevant, they are chosen because they can model the characteristics of the Ultracapacitor with high accuracy [27].

This paper proposes a SOC estimation method using the Adaptive Neuro-Fuzzy Inference System (ANFIS) algorithm from various models with their respective levels of complexity. Artificial neural networks can form models in patterns such as neural networks obtained through learning experimental data to form a learning set as a system representation with a minimal error value by calculating the mean square error [28]. The learning stage of the artificial neural network is proven to have high accuracy and is relevant to be applied in various advanced research in the presence of appropriate data for the actual condition of the system [29]. The SOC estimation method, which is performed by predicting the Neural Network algorithm and in collaboration with the reasoning owned by the Fuzzy Inference System, has a high level of accuracy [30][31]. The learning and training processes make ANFIS one of the best methods for estimating the SOC Ultracapacitor, which has dynamic behavior [32].

The experiment in this paper uses the equivalent circuit model (ECM) as the Ultracapacitor characteristic modeling, while the ANFIS method is used as the SOC estimation method. In addition, direct testing will be carried out on the hardware with constant current charging and discharging with a load in the form of a DC electronic load to obtain validation of the actual condition of the Ultracapacitor. The results obtained will be compared between theoretical calculations with an equivalent circuit model, SOC estimation using the ANFIS, and experimental data conducted in the laboratory.

II. Materials and Methods

A. Ultracapacitor modeling

A series resistor and capasitor (RC) circuit is the simplest form of modeling the equivalent circuit model applied to an Ultracapacitor. This model consists of a resistor representing the internal resistance and a capacitor indicating the charge capacity during charging and discharging of the Ultracapacitor. Figure 1 shows the simple modeling of an Ultracapacitor with an equivalent circuit model.

Based on the Ultracapacitor equivalent circuit's modeling, the following equations (1) and (2) are obtained based on Kirchhoff's voltage law. V_t is the terminal voltage obtained by measuring the voltage, v_c is the authentic voltage of the Ultracapacitor, i is

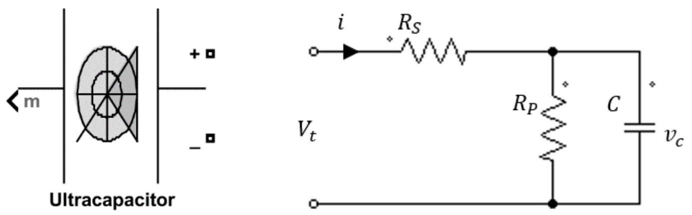

(a) (b)

Figure 1. (a) Ultracapacitor library in MATLAB; (b) Proposed ultracapacitor modeling

the current in charge and discharge conditions, and R_s is the equivalent series resistance of the Ultracapacitor.

$$V_t = v_c + i \cdot R_s \tag{1}$$

$$v_c = V_t - i \cdot R_s \tag{2}$$

Ultracapacitor modeling primarily aims to simulate the characteristics under charge and discharge conditions. The change in terminal voltage during the Ultracapacitor's service life indicates the charging and discharging process. The advantages of using Ultracapacitors as energy storage devices are their ability to store energy long-term and high output power. In addition to the Ultracapacitor operating conditions, the terminal voltage can slowly decrease due to self-discharge. Self-discharge is caused by two conditions: ion diffusion and leakage current.

This paper uses five Ultracapacitor units in series for a higher nominal voltage with a lower capacitance. Table 1 shows the data of the Ultracapacitors used in this research. Table 1 mentions the datasheet as an initial reference for the internal parameters of the Ultracapacitor in the SOC estimation on the Simulink. In the advanced stage, this data will be validated through testing by researchers to determine the actual value of the internal parameters so that the SOC estimate follows the actual conditions to be applied to Simulink and the designed Ultracapacitor hardware.

The parameter values of the Ultracapacitor components used in this paper are based on the SAMWHA Ultracapacitor datasheet. The following equation can validate parameter values based on the tests performed. The following equation can be used to determine the equivalent parallel resistance (R_p) value. C is the capacitance of Ultracapacitors, V_1 is the initial voltage, and V_2 is the final voltage after charging.

$$R_p = \frac{-10800}{ln\ (V_2/V_1)\ C} \tag{3}$$

In this model, the aim is to find out the value of the Ultracapacitor parameters that are not listed in the datasheet in this paper, namely the equivalent parallel resistance, which has been described in equation (3), and to validate the actual value of equivalent series resistance and capacitance. To determine the value of equivalent series resistance, equation (4) can be used, where ΔV is the change in voltage from the charging state to the open-circuit voltage and ΔI is the current value used in the testing process.

$$R_s = \frac{\Delta V}{\Delta I} \tag{4}$$

Then, the stored charge approximation method determines the capacitance (C), as shown in equation (5). The ΔV value is the subtraction between V_1 and V_2. V_1 is a voltage of 0.8 of the nominal voltage of the ultracapacitor. Meanwhile, V_2 is a voltage of 0.4 of the nominal voltage of the Ultracapacitor. The value of ΔQ calculates the current integral during the testing process, where t_1 is the discharge time to reach V_1 and t_2 is the discharge time to reach V_2.

$$C = \frac{\Delta Q}{\Delta V} = \frac{\int_{t_1}^{t_2} I(t)dt}{(V_1 - V_2)} \tag{5}$$

B. State of charge estimation

The state of charge is the ratio between an energy storage device's total usable energy capacity. This research is the ratio of the available energy capacity to the total charge in the Ultracapacitor. State of Charge represents the available energy and is generally expressed as a percentage in 0 to 1 or 0 to 100 %, with 100 % indicating the Ultracapacitor is complete and 0 % is empty. The SOC is an important parameter that must be known in using energy storage in addition to the voltage, current, capacity, and energy value. State of charge monitoring is necessary to maintain the Ultracapacitor's lifetime by avoiding the risk of overcharging and over-discharging, which can affect the structural components of the Ultracapacitor. At a more advanced stage, the determination of the SOC can be used to control energy use. The accuracy level of SOC estimation on the level of measurement accuracy and the suitability of the modeling to get an estimate that follows the actual conditions of the Ultracapacitor. Based on the equivalent circuit model

Table 1.
Ultracapacitor datasheet

Parameter	Value	Unit
Rated voltage	2.7	Volt
Capacitance	500	Farad
Cycle life	500000	Cycle
Lifetime	10	Year
ESR	3.1	mΩ
Maximum continuous current	25	Ampere
Maximum peak current	264.7	Ampere
Specific energy	5.59	Wh/kg
Mass	89	Grams
Operating temperature	-40° to 65°	Celcius

modeling, the formula to determine the SOC on the Ultracapacitor can be used with the following formula.

$$SOC\ \% = \left[\frac{v_c}{v_{c\,max}}\right] \times 100 \quad (6)$$

In equation (6), the value of v_c is the Ultracapacitor voltage obtained from the modeling results using an equivalent circuit model. For $v_{c\,max}$ is the value of v_c at the maximum point in the charging process. The following summary in Table 2 compares the methods used to estimate SOC on Ultracapacitors, along with their advantages and disadvantages. The table describes each method used for estimating the SOC Ultracapacitor and its ability to get estimation results that follow actual conditions, which are described as advantages and an explanation of the disadvantages of the methods used in the paper in actual application.

C. Adaptive neuro-fuzzy inference system (ANFIS)

The research presented in this paper used the ANFIS to estimate the SOC of Ultracapacitor. The advantages possessed by artificial neural networks and fuzzy inference systems are collaborating to form ANFIS. With the ability to learn through data learning and fuzzy inference system reasoning, ANFIS is considered to work optimally to estimate the SOC on the ultracapacitor. The ANFIS architecture has five layers with different special functions to form a pattern based on the training results. Figure 2 shows that each layer has its function, which will be estimated using the ANFIS algorithm through detailed calculations to get a pattern that fits the model [33]. ANFIS is an advanced application of a fuzzy inference system with neural network architecture using Takagi-Sugeno as a learning process and determining the desired form of membership function. The ANFIS architecture consists of five layers with different special functions in each layer, making ANFIS performance with more complex and detailed processing. There are two rules for processing ANFIS with if-then rules as in equations (7) and (8).

Rule 1: if x is A_1 and y is B_1 then $f_1 = p_1x + q_1y + r_1$ (7)

Rule 2: if x is A_2 and y is B_2 then $f_2 = p_2x + q_2y + r_2$ (8)

A_1, A_2, B_1, and B_2 are the premise parameters of the input membership functions x and y, while p_1, q_1, r_1, p_2, q_2, and r_2 are linear consequent parameters of the Takagi-Sugeno fuzzy inference system. In designing ANFIS, it is necessary to pay attention to two rules in equations (7) and (8), clustering rules for data learning so that data processing at each layer follows the training data formed. In addition, it is necessary to pay attention to several important aspects, namely the type of membership function, the number of membership functions, error tolerance, and the number of epochs in the training process. The following is the workflow of the five layers in ANFIS.

1) Layer 1

The fuzzification layer at node i for μA and μB is shown in equations (9) and (10). Each neuron is adaptive to the parameters to generate a membership function. At input, x will form μA_i, and input y will form μB_i with i =1,2 where 1 and 2 are two conditions resulting from clustering

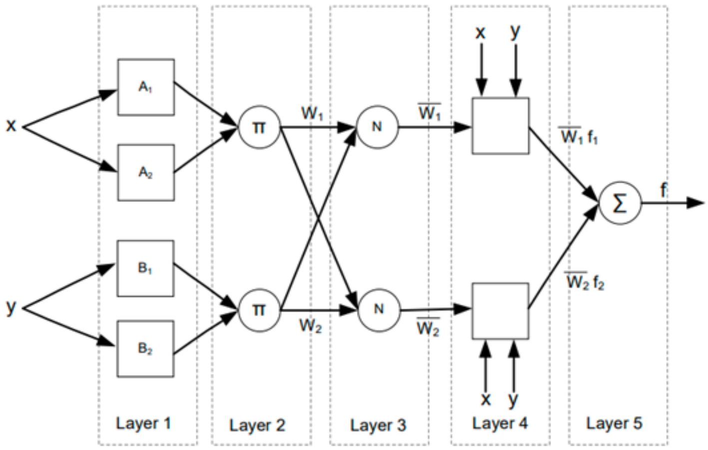

Figure 2. ANFIS Architecture [33]

Table 2.
Advantages and disadvantages of SOC methods

Methods	Advantage	Disadvantage
Open-circuit voltage [1]	Simple and easy	Ultracapacitors need long times of rest to achieve voltage stability, causing difficulties in measurements.
Coulomb counting [1]	Simple and easy	Inaccurate current measurement will cause SOC estimation error, and the error will increase with long-term accumulation.
Extended Kalman Filter [2]	High accuracy despite external interference	This method cannot be applied directly to estimate the states of a non-linear system.
Open-circuit voltage – UKF [20]	High accuracy	Requires Ultracapacitor modeling, OCV, and UKF equations to get accurate results.
Kalman Filter [22]	High accuracy	Estimation errors must be recalculated to get convergent results.

membership function fuzzy logic reasoning to determine membership function.

$$O_i^1 = \mu A_i(x)\,, \quad i = 1{,}2 \tag{9}$$

$$O_i^1 = \mu B_i(y)\,, \quad i = 1{,}2 \tag{10}$$

2) Layer 2

The fixed node layer w_i produces output in the form of multiplication of all incoming signals by the node, representing the activation of the fuzzy rule. Equation (11) shows the multiplication of w_i using μA_i and μB_i with i for conditions 1 and 2, which have been formed in the previous layer.

$$O_i^2 = w_i = \mu A_i(x) \cdot \mu B_i(y), \quad i = 1{,}2 \tag{11}$$

3) Layer 3

The nonadaptive normalization layer performs an activation function. $\overline{w_i}$ is a normalization of the fuzzy rule activation form with the value of w_i divided by the total values of w_1 and w_2. Determination of the value at layer 3 is shown in equation (12).

$$O_i^3 = \overline{w_i} = \frac{w_i}{w_1 + w_2}\,, \quad i = 1{,}2 \tag{12}$$

4) Layer 4

The adaptive defuzzification layer for $\overline{w_i}$ is multiplied by p_i , q_i , and r_i . $\overline{w_i} f_i$ is useful for denormalizing the values obtained at layer 3. To get the parameter values for the coefficients of p_i, q_i, and r_i with i for 1 and 2, using the Recursive Least Square Estimator (RLSE) calculation. The following equation (13) is used to get the value on layer 4.

$$O_i^4 = \overline{w_i} f_i = \overline{w_i} \cdot [(p_i \cdot x) + (q_i \cdot y) + r_i)], \quad i = 1{,}2 \tag{13}$$

5) Layer 5

The single fuzzy node output layer is fixed to return all outputs by adding up all the inputs obtained from the fourth layer to determine the output layer using the function in equation (14). In the final calculation, layer 5 is obtained from the output layer 4 from the results of $\overline{w_i} f_i$. The output from layer 5 is the estimated value of the Ultracapacitor's authentic voltage, which will be used as the main parameter for SOC estimation using the ANFIS algorithm.

$$O_i^5 = \sum \overline{w_i} f_i = \frac{\sum w_i \cdot f_i}{\sum f_i}, \quad i = 1{,}2 \tag{14}$$

III. Results and Discussions

In this experiment, the Ultracapacitor energy storage system will be tested for charging using a DC Power Supply and discharging using a DC electronic load with a variable current to model the actual conditions in a non-linear load. Figure 3 shows a research diagram for estimating SOC. The equivalent circuit model in Figure 1 and equation (6) in this system is used as true SOC because it is an application of estimation with modeling to determine open-circuit voltage, which is commonly used for SOC estimation in addition to coulomb counting. While the system is running, the measured voltage is the charging voltage. Estimating the authentic voltage on the Ultracapacitor obtained through modeling for estimation using the open-circuit voltage method is necessary. The authentic voltage on the Ultracapacitor is the essential parameter to determine the state of charge. In simple terms, it is the authentic voltage of the Ultracapacitor without the influence of equivalent series resistance. In this paper, five Ultracapacitor units are used in series with the simulation on Simulink MATLAB and hardware testing of measuring terminal voltage and current under charge and discharge conditions.

The data required is the measurement of current and voltage at the terminal of the Ultracapacitor energy storage system. The Ultracapacitor is mathematically analyzed to adjust the electrical behavior and estimate the SOC with a modeling system based on the equivalent circuit model. RC circuit in series with a parallel resistor as a self-discharge model, as shown in Figure 1. The ANFIS built will be used as an estimator to determine the SOC value from the results of the supervised learning. The data obtained from the logging results will be processed simultaneously through modeling and the ANFIS estimator. Performance testing will be performed using the root mean square error (RMSE), mean square error (MSE), mean absolute error

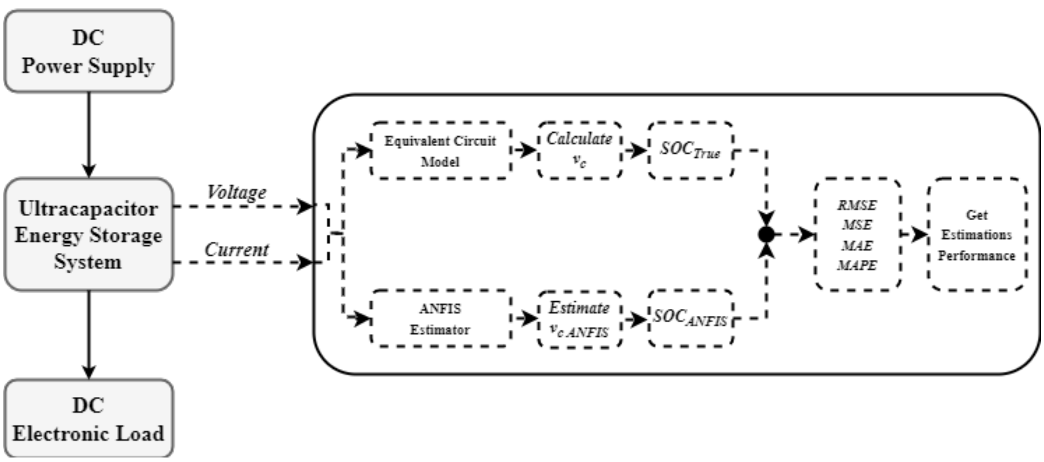

Figure 3. Block diagram of the comparative analysis estimations SOC

(MAE), and mean absolute percentage error (MAPE) methods.

From the results of characteristic testing with varying current patterns on charging and discharging conditions that have been carried out on Ultracapacitor energy storage, training will be carried out on the ANFIS toolbox to build a Fuzzy Inference System. The required training data are voltage and current on charging and discharging conditions, with the target data being the authentic voltage on the Ultracapacitor. The training process from the data obtained from testing the Ultracapacitor characteristics is carried out on the MATLAB toolbox. Figure 4 shows the training results using a hybrid method to get an algorithm following the original system. ANFIS training is used to form a fuzzy inference system pattern in the estimation process through the learning process. A hybrid method of artificial neural networks is used to form a network pattern that is appropriate and adaptive to system performance that varies with charging and discharging conditions.

The flowchart of the ANFIS architecture is shown in Figure 5. There are a series of processes, so the mechanism can work optimally according to the expected target. In the early stages, there is data sharing for training and testing, for training data using data from test results with the patterned current. In comparison, testing data using data from tests with random currents. Based on the results of the ANFIS development, the average testing error of $6.9917e^{-9}$ indicates optimal learning outcomes and is following the desired target.

A. Simulation results

From the training and data testing results to building ANFIS, performance testing is carried out on charging and discharging conditions in the simulation. Current sources are randomly assigned to check the capability of the ANFIS as an estimator.

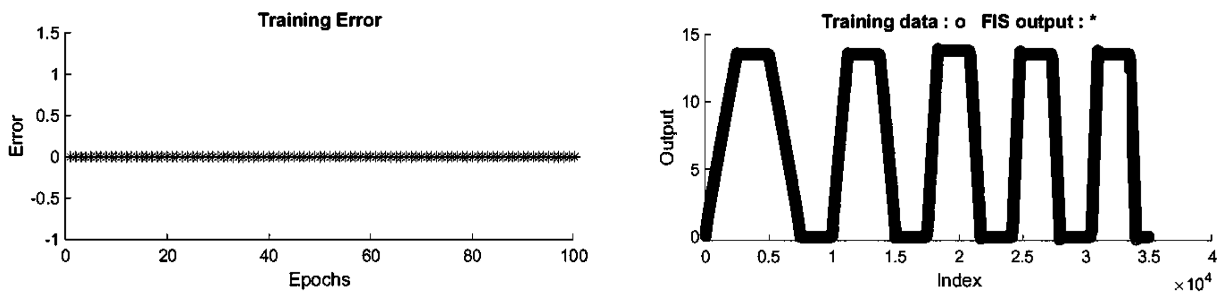

Figure 4. (a) Training error with 100 epochs; (b) Training data with authentic ultracapacitor voltage as target

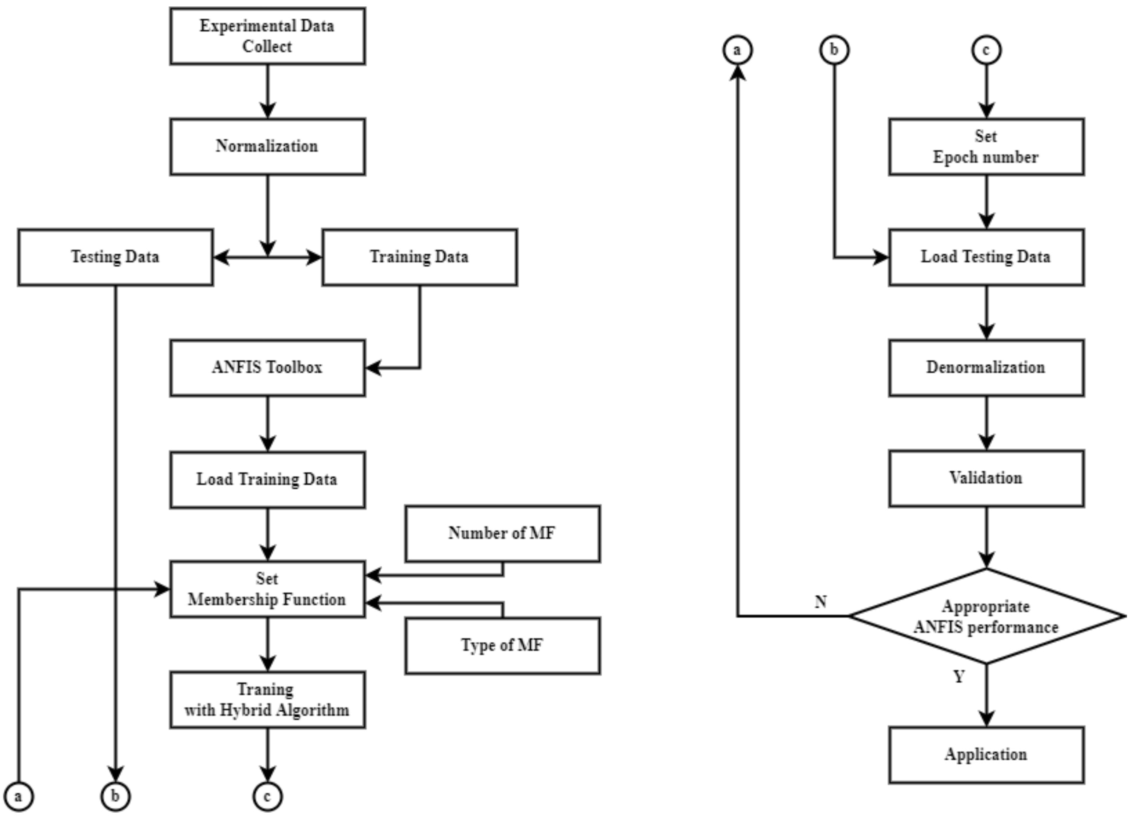

Figure 5. Flowchart of ANFIS architecture

In this simulation, the capacitance value of 100 farads and the equivalent series resistance of five Ultracapacitor units of 15.5 mΩ is determined based on the reference obtained from the datasheet. Figure 6 shows the charging and discharging process plot results in MATLAB.

In the results, the variation of the membership function is conducted to determine the most optimal ANFIS performance for SOC estimation (Figure 7). The charging and discharging currents are made similar to the actual conditions in using non-linear loads to test the estimator's performance under conditions with drastic changes. Over time, the SOC will increase when charging and decrease when discharging. An Ultracapacitor can handle this condition because it has a high discharge rate, a wide operating temperature, and a long lifecycle, making it safe to use in extreme conditions.

Table 3 shows the calculation of ANFIS performance testing using the RMSE, MSE, MAE, and MAPE methods and the results of three different membership functions to determine the best model for the ANFIS estimator. Based on the test, ANFIS has a high accuracy performance with MAPE calculation error values of 0.70 % in charging conditions and 0.83 % in discharging conditions for actual data compared to the estimated equivalent circuit modeling. The accuracy level is excellent if the prediction data is close to the actual data. The blue graph shows the true SOC obtained using equation (6) from the estimation results. The true SOC will compare the ANFIS estimator shown in the red graph for the triangular membership function, the yellow graph for the trapezoidal membership function, and the green graph is the gaussian membership function. Table 4 shows the results of

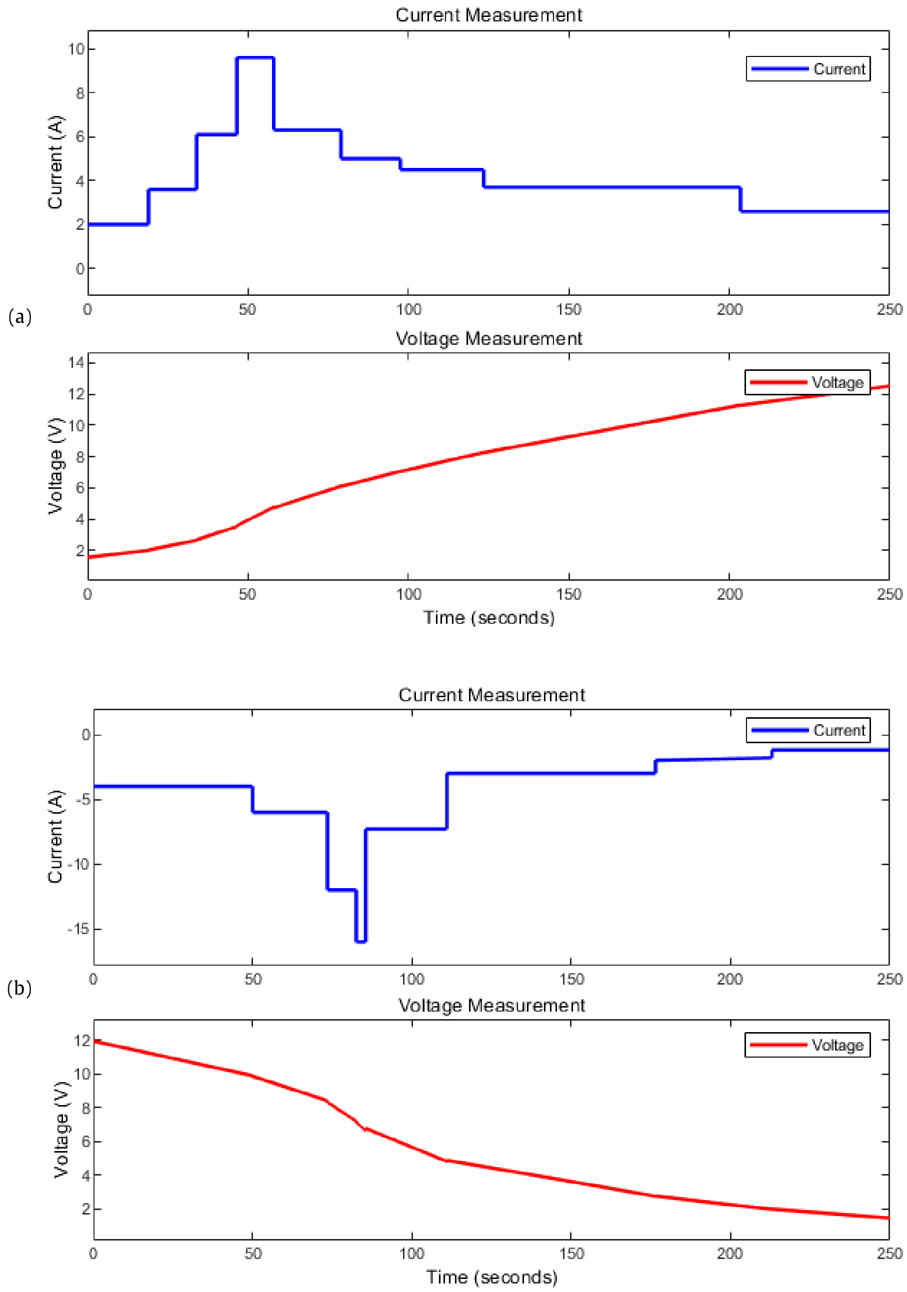

Figure 6. (a) Charging Current and Voltage; (b) Discharging Current and Voltage

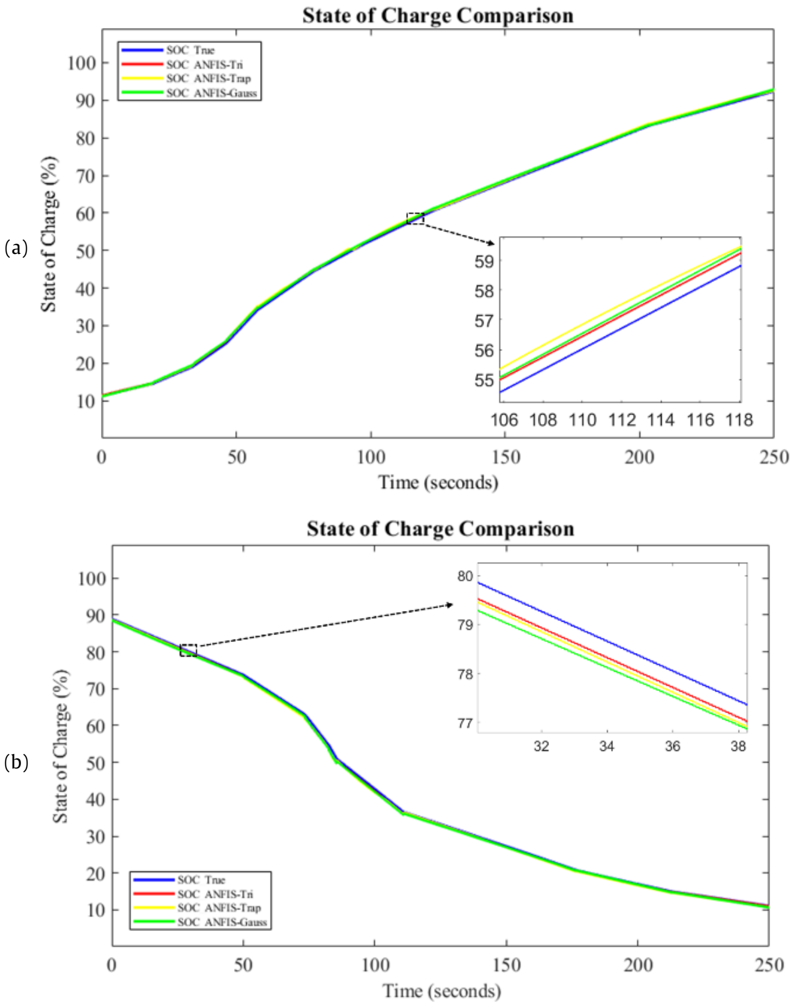

Figure 7. (a) Estimations SOC ANFIS with various MF on charging; (b) Estimations SOC ANFIS with various MF on discharge

Table 3.
Comparison estimation SOC with various membership functions

ANFIS membership function	RMSE		MSE		MAE		MAPE	
	Charge	Discharge	Charge	Discharge	Charge	Discharge	Charge	Discharge
Triangular	0.0201377	0.0198281	0.0004055	0.0003932	0.0004027	0.0003965	0.7085133	0.8398471
Trapezoidal	0.0201625	0.0197755	0.0004065	0.0003911	0.0004032	0.0003954	0.8328958	1.1025848
Gaussian	0.0201474	0.0197879	0.0004059	0.0003916	0.0004029	0.0003957	0.7569106	1.0405872

Table 4.
Comparison with previous research

Methods	Average error	
	Charge	Discharge
ECM-EKF [2][22]	<5.00 %	<5.00 %
ECM-ANFIS	0.99 %	0.92 %

calculating the average error value in the SOC estimation with previous research using the equivalent circuit model. The SOC estimation research using ANFIS showed better results than the Extended Kalman Filter method.

B. Experimental results

This research uses a hardware design, as shown in Figure 8, with the results presented using MATLAB to determine the performance of ANFIS for estimating the state of charge. Observation of voltage and current on charging and discharging conditions using the Yokogawa DL-3031 Oscilloscope with programmable DC power supply, which functions as a charger, and DC electronic load as a load that works to represent use as energy storage in electric vehicles and other electrical applications.

The charging uses constant current from programmable DC power supply mode by testing various current values to obtain varying charging conditions. Ultracapacitor charging on real hardware was taken using a Yokogawa DL-3031 Oscilloscope with an increase in terminal voltage from the initial condition to full 13.5 Volts and a variable constant current. From the characteristic test carried out with the results in Figure 9, a calculation analysis can be carried out to determine the internal parameters of the Ultracapacitor with equation (3) to determine the value of equivalent parallel resistance, equation (4) to determine the value of equivalent series

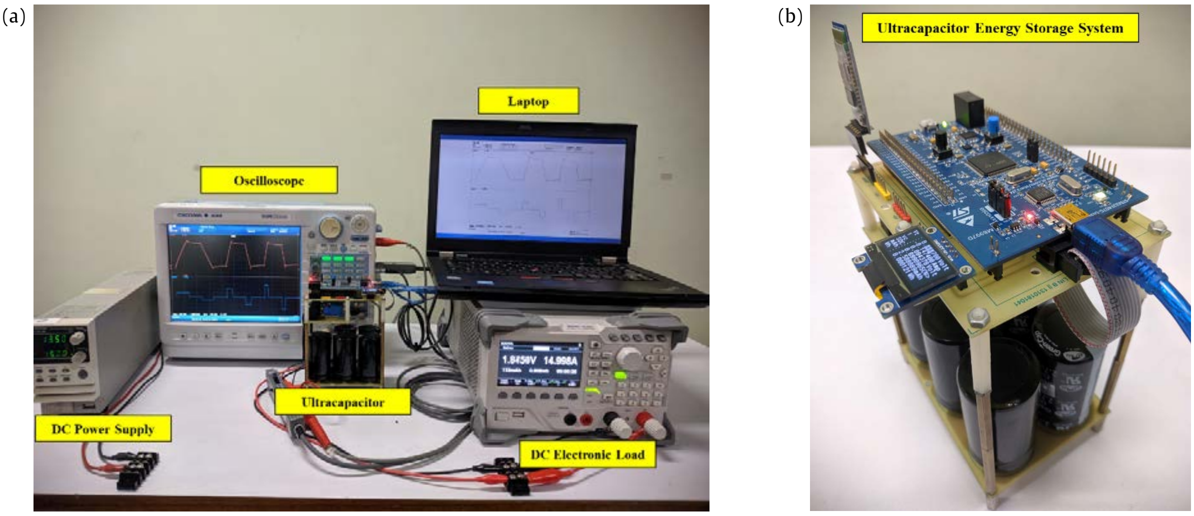

Figure 8. (a) Experimental setup; (b) Ultracapacitor energy storage system

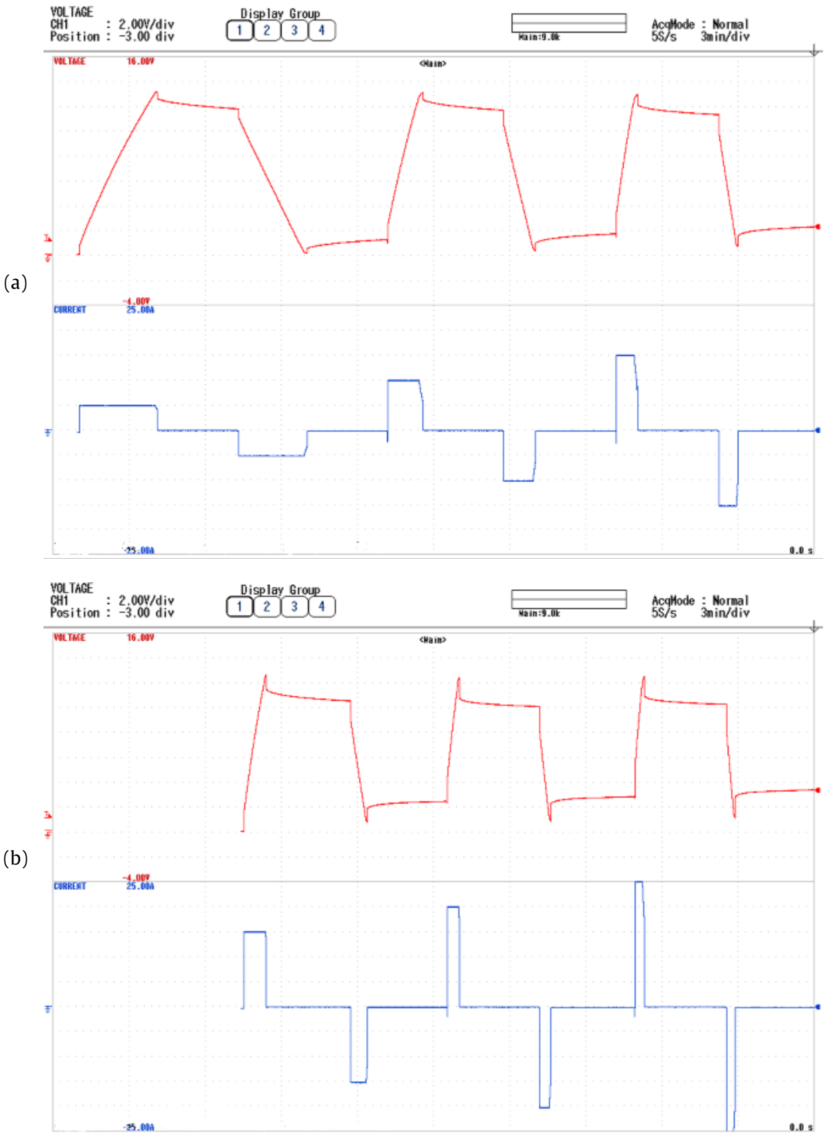

Figure 9. Ultracapacitor characteristic testing (a) 5A, 10 A, and 15 A testing; (b) 15 A, 20 A, and 25 A testing

resistance, and equation (5) to determine the value of capacitance.

Based on the characteristic test data shown in Table 5 with the variation of the current source, it is known that the average value of equivalent series resistance (R_s) is 0.10828 Ω, equivalent parallel resistance (R_p) 26.006 Ω, and capacitance (C) 80.748 Farads. Changes in the capacitance value from its

Table 5.
Ultracapacitor parameter value from characteristic test results

Charging current	R_s	R_p	C
5 A	0.1266	30.04	80.91
10 A	0.1147	25.11	81.35
15 A	0.1066	24.15	80.19
20 A	0.0970	25.15	81.29
25 A	0.0965	25.58	80

original condition can be caused by being degraded due to use. Meanwhile, the value of R_s can is caused by the connecting conductor on each Ultracapacitor. After testing the characteristics and getting actual parameters on the hardware, testing is carried out to determine the success of the estimation process. Current sources with varying random values are used for the charging process to determine the ANFIS capability built to accurately estimate the SOC value. Figure 10 is a charging process with a random current, making the voltage increase in the Ultracapacitor non-linear. Therefore, ANFIS can be relied on to handle these conditions.

Figure 11 shows that the estimation graph using ANFIS with three different membership functions has results that coincide with true SOC conditions. However, out of the three ANFIS membership functions used, the triangular membership function has the most superior performance, with the lowest MAPE at 0.76 %.

In Figure 12, the following data is presented for the calculation of RMSE, MSE, MAE, and MAPE from the comparison between the true SOC value and the estimated SOC using various ANFIS membership functions.

Based on hardware experiments, the results of the error calculation using the RMSE, MSE, MAE, and MAPE methods are shown to determine the performance of ANFIS in estimating the state of

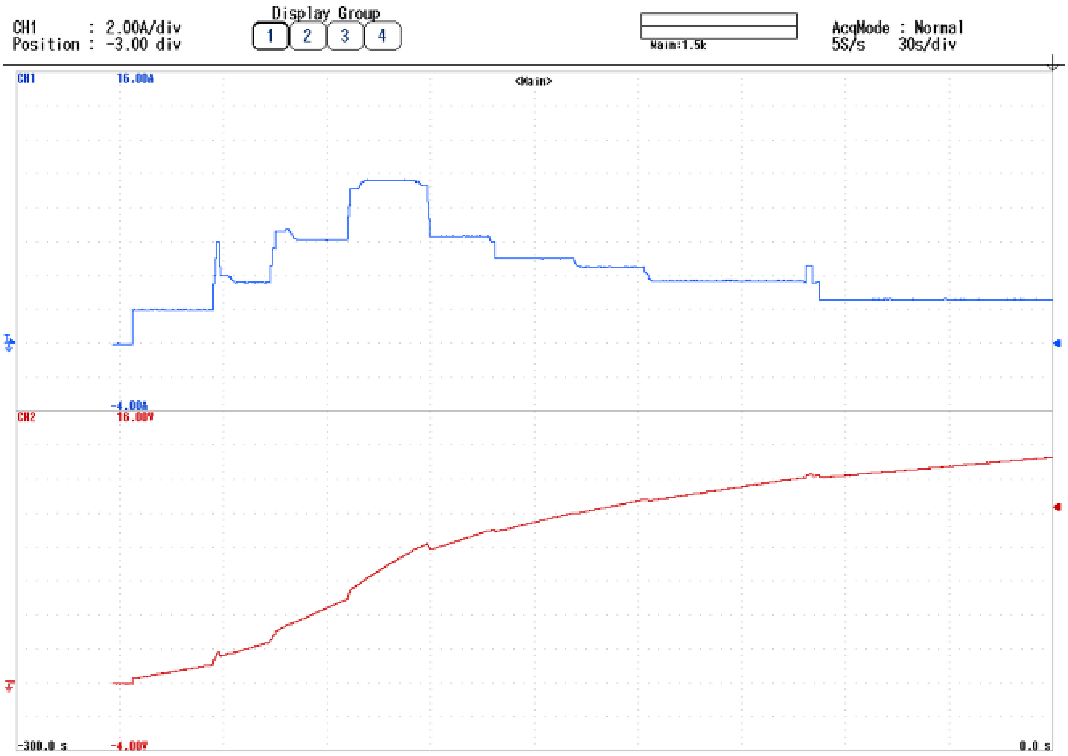

Figure 10. Charging current (top) and voltage (bottom)

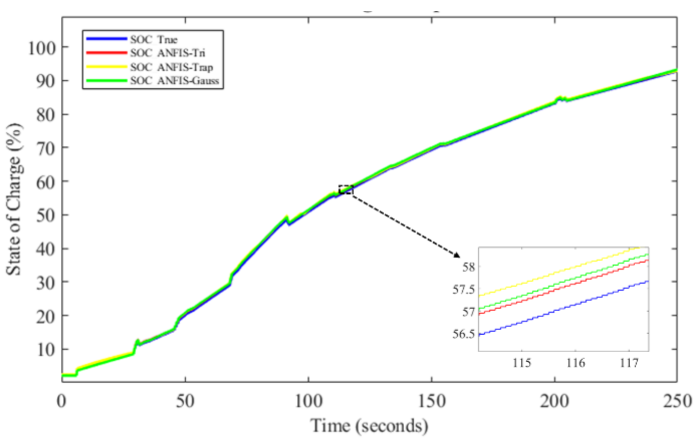

Figure 11. Estimations of SOC ANFIS with various MF

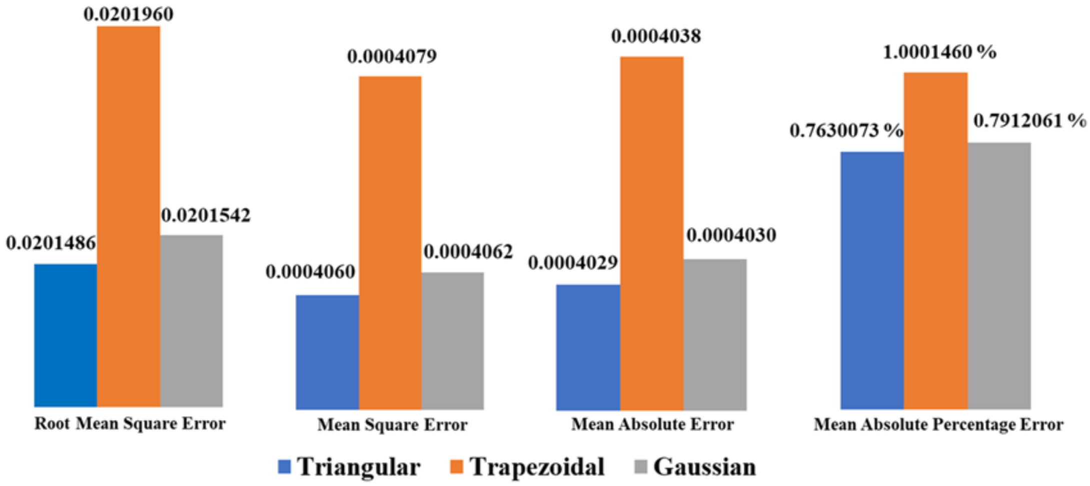

Figure 12. SOC estimation error values with method calculations: RMSE, MSE, MAE, and MAPE

charge on the ultracapacitor. The chart above is the result of a comparison of the estimation results by ANFIS with three different memberships, namely triangular, trapezoidal, and gaussian, to determine the most efficient form of membership function in the estimation process. The blue chart represents the performance of the triangular membership function, the orange chart represents the performance of the trapezoidal membership function, and the gray chart represents the performance of the gaussian membership function from the error calculation results using the four relevant methods used as a reference to determine learning performance.

IV. Conclusion

Based on the research results to estimate SOC, the equivalent circuit model is a relevant circuit for Ultracapacitor modeling because it has a simple and accurate model. It is also supported by ANFIS intelligence as an estimator capable of estimating the SOC value with high accuracy. ANFIS with triangular membership function as a method for predicting SOC estimation on ultracapacitors works optimally and has high accuracy with MAPE calculation of 0.70 % for charging while 0.83 % for discharging compared to true SOC. While in the hardware experiment, the results of the SOC estimation with the triangular membership function are small at 0.76 %. It is hoped that SOC research can develop with simplification and better performance in the future. Ultracapacitors as energy storage devices, both hybrid and primary, can be developed and applied to electric vehicles and other electronic applications because of their excellent performance.

Acknowledgment

The authors are grateful to Politeknik Elektronika Negeri Surabaya and Renewable Energy Laboratory for the permission to use the Ultracapacitor for this research and to publish this paper. We would also like to thank those who have helped and supported us in preparing this manuscript.

Declarations

Author contribution

Rizal Nurdiansyah: Writing - Original Draft, Writing - Review & Editing, Conceptualization, Software, Hardware, Formal analysis, Investigation, Visualization, Validation. Novie Ayub Windarko: Writing - Original Draft, Formal analysis, Conceptualization, Investigation, Visualization, Validation, Data Curation, Resources, Supervision. Renny Rakhmawati: Formal analysis, Conceptualization, Investigation, Supervision. Muhammad Abdul Haq: Formal analysis, Supervision.

Funding statement

This research did not receive any specific grant from funding agencies in the public, commercial, or not-for-profit sectors.

Competing interest

The authors declare that they have no known competing financial interests or personal relationships that could have appeared to influence the work reported in this paper.

Additional information

Reprints and permission: information is available at https://mev.lipi.go.id/.

Publisher's Note: National Research and Innovation Agency (BRIN) remains neutral with regard to jurisdictional claims in published maps and institutional affiliations.

References

[1] C. Liu, Q. Li, and K. Wang, "State-of-charge estimation and remaining useful life prediction of supercapacitors," *Renew. Sustain. Energy Rev.*, vol. 150, p. 111408, Oct. 2021.

[2] A. Afandi, B. Sumantri, and N. A. Windarko, "Estimation state of charge (SOC) of Ultracapacitor based on classical equivalent circuit using Extended Kalman Filter," in *2020 International Electronics Symposium (IES)*, Surabaya, Indonesia, Sep. 2020, pp. 31–36.

[3] P. Fornaro, P. Puleston, and P. Battaiotto, "On-line parameter estimation of a Lithium-Ion battery/supercapacitor storage system using filtering sliding mode differentiators," *J. Energy Storage*, vol. 32, p. 101889, Dec. 2020.

[4] K. Alobeidli and V. Khadkikar, "A new Ultracapacitor state of charge control concept to enhance battery lifespan of dual storage electric vehicles," *IEEE Trans. Veh. Technol.*, vol. 67, no. 11, pp. 10470–10481, Nov. 2018.

[5] T. Rout, A. Chowdhury, M. K. Maharana, and S. Samal, "Analysis of energy management system for photovoltaic

system with battery and supercapacitor using fuzzy logic controller," in *2018 Technologies for Smart-City Energy Security and Power (ICSESP)*, Bhubaneswar, Mar. 2018, pp. 1–4.

[6] A. Amin, K. Ismail, and A. Hapid, "Implementation of a LiFePO4 battery charger for cell balancing application," *J. Mechatron. Electr. Power Veh. Technol.*, vol. 9, no. 2, p. 81, Dec. 2018.

[7] B. Traore, M. Doumiati, C. Morel, J.-C. Olivier, and O. Soumaoro, "Energy management strategy based on a new adaptive filtering algorithm for battery-ultracapacitor electric vehicles," in *2020 15th IEEE Conference on Industrial Electronics and Applications (ICIEA)*, Kristiansand, Norway, Nov. 2020, pp. 392–396.

[8] A. R. Al Tahtawi and A. S. Rohman, "Simple supercapacitor charging scheme of an electric vehicle on small-scale hardware simulator: a prototype development for education purpose," *J. Mechatron. Electr. Power Veh. Technol.*, vol. 7, no. 2, pp. 77–86, Dec. 2016.

[9] H. Yang, "Estimation of supercapacitor charge capacity bounds considering charge redistribution," *IEEE Trans. Power Electron.*, vol. 33, no. 8, pp. 6980–6993, Aug. 2018.

[10] Q. Zhu *et al.*, "A new view of supercapacitors: Integrated supercapacitors," *Adv. Energy Mater.*, vol. 9, no. 36, p. 1901081, Sep. 2019.

[11] H. Jiang, L. Xu, J. Li, Z. Hu, and M. Ouyang, "Energy management and component sizing for a fuel cell/battery/supercapacitor hybrid powertrain based on two-dimensional optimization algorithms," *Energy*, vol. 177, pp. 386–396, Jun. 2019.

[12] I. Jarraya, F. Masmoudi, M. H. Chabchoub, and H. Trabelsi, "An online state of charge estimation for Lithium-ion and supercapacitor in hybrid electric drive vehicle," *J. Energy Storage*, vol. 26, p. 100946, Dec. 2019.

[13] S. Hussain, M. U. Ali, G.-S. Park, S. H. Nengroo, M. A. Khan, and H.-J. Kim, "A real-time bi-adaptive controller-based energy management system for battery–supercapacitor hybrid electric vehicles," *Energies*, vol. 12, no. 24, p. 4662, Dec. 2019.

[14] C-T. Ma, "Design and implementation of a hybrid real-time state of charge estimation scheme for battery energy storage systems," *Processes*, vol. 8, no. 1, p. 2, Dec. 2019.

[15] H. Yang, "Application of Peukert's law in supercapacitor discharge time prediction," *J. Energy Storage*, vol. 22, pp. 98–105, Apr. 2019.

[16] P. Venugopal, "State-of-charge estimation methods for li-ion batteries in electric vehicles," *International Journal of Innovative Technology and Exploring Engineering (IJITEE)*, vol. 8, no. 7, p. 11, 2019.

[17] Poonam, K. Sharma, A. Arora, and S. K. Tripathi, "Review of supercapacitors: Materials and devices," *J. Energy Storage*, vol. 21, pp. 801–825, Feb. 2019.

[18] H. Chaoui and H. Gualous, "Online lifetime estimation of supercapacitors," *IEEE Trans. Power Electron.*, vol. 32, no. 9, pp. 7199–7206, Sep. 2017.

[19] L. Rozaqi, E. Rijanto, and S. Kanarachos, "Comparison between RLS-GA and RLS-PSO for Li-ion battery SOC and SOH estimation: a simulation study," *J. Mechatron. Electr. Power Veh. Technol.*, vol. 8, no. 1, pp. 40–49, Jul. 2017.

[20] P. Saha, S. Dey, and M. Khanra, "Accurate estimation of state-of-charge of supercapacitor under uncertain leakage and open circuit voltage map," *J. Power Sources*, vol. 434, p. 226696, Sep. 2019.

[21] M. A. Awadallah and B. Venkatesh, "Accuracy improvement of SOC estimation in lithium-ion batteries," *J. Energy Storage*, vol. 6, pp. 95–104, May 2016.

[22] Z. Tao, G. Shaoting, L. Xin, and J. Jing, "SOC estimation scheme of super capacitor based on Calman filter," in *2016 IEEE 11th Conference on Industrial Electronics and Applications (ICIEA)*, Hefei, China, Jun. 2016, pp. 918–921.

[23] J. Wang, L. Zhang, J. Mao, J. Zhou, and D. Xu, "Fractional order equivalent circuit model and SOC estimation of supercapacitors for use in HESS," *IEEE Access*, vol. 7, pp. 52565–52572, 2019.

[24] J. I. Hidalgo-Reyes, J. F. Gómez-Aguilar, R. F. Escobar-Jiménez, V. M. Alvarado-Martínez, and M. G. López-López, "Classical and fractional-order modeling of equivalent electrical circuits for supercapacitors and batteries, energy management strategies for hybrid systems and methods for the state of charge estimation: A state of the art review," *Microelectron. J.*, vol. 85, pp. 109–128, Mar. 2019.

[25] L. Zhang, X. Hu, Z. Wang, F. Sun, and D. G. Dorrell, "A review of supercapacitor modeling, estimation, and applications: A control/management perspective," *Renew. Sustain. Energy Rev.*, vol. 81, pp. 1868–1878, Jan. 2018.

[26] M. R. Djalal, H. Setiadi, and A. Imran, "Frequency stability improvement of micro hydro power system using hybrid SMES and CES based on Cuckoo search algorithm," *J. Mechatron. Electr. Power Veh. Technol.*, vol. 8, no. 2, pp. 76–84, Dec. 2017.

[27] M. E. Şahin, F. Blaabjerg, and A. Sangwongwanich, "Modelling of supercapacitors based on simplified equivalent circuit," *CPSS Trans. Power Electron. Appl.*, vol. 6, no. 1, pp. 31–39, Mar. 2021.

[28] M. Rif'an, F. Yusivar, and B. Kusumoputro, "Sensorless-BLDC motor speed control with ensemble Kalman filter and neural network," *J. Mechatron. Electr. Power Veh. Technol.*, vol. 10, no. 1, pp. 1–6, Dec. 2019.

[29] K. Faqih, S. Sujito, S. Sendari, and F. S. Aziz, "Smart guided missile using accelerometer and gyroscope based on backpropagation neural network method for optimal control output feedback," *J. Mechatron. Electr. Power Veh. Technol.*, vol. 11, no. 2, pp. 55–63, Dec. 2020.

[30] A. Soualhi *et al.*, "Heath monitoring of capacitors and supercapacitors using the neo-fuzzy neural approach," *IEEE Trans. Ind. Inform.*, vol. 14, no. 1, pp. 24–34, Jan. 2018.

[31] A. Fotouhi, D. J. Auger, K. Propp, and S. Longo, "Lithium–sulfur battery state-of-charge observability analysis and estimation," *IEEE Trans. Power Electron.*, vol. 33, no. 7, pp. 5847–5859, Jul. 2018.

[32] K. V. Singh, H. O. Bansal, and D. Singh, "Hardware-in-the-loop implementation of ANFIS based adaptive SoC estimation of lithium-ion battery for hybrid vehicle applications," *J. Energy Storage*, vol. 27, p. 101124, Feb. 2020.

[33] H. Suryoatmojo, M. Ridwan, D. C. Riawan, E. Setijadi, and R. Mardiyanto, "Hybrid particle swarm optimization and recursive least square estimation based ANFIS multioutput for BLDC motor speed controller," *International Journal of Innovative Computing, Information and Control (ICIC)*, vol. 15, no. 3, June 2019.